Acta Oceanol. Sin., 2017, Vol. 36, No. 9, P. 45–51
DOI: 10.1007/s13131-017-1110-3
http://www.hyxb.org.cn
E-mail: hyxbe@263.net

A case study of the consistency problem in the inverse estimation

WEI Yanzhou[1, 2, 3*], KANG Xianbiao[2, 4], PEI Yuhua[1]

[1] State Key Laboratory of Satellite Ocean Environment Dynamics, Second Institute of Oceanography, State Oceanic Administration, Hangzhou 310012, China

[2] Key Laboratory of Ocean Circulation and Waves, Institute of Oceanology, Chinese Academy of Sciences, Qingdao 266071, China

[3] University of Chinese Academy of Sciences, Beijing 100049, China

[4] College of Air Traffic Management, Civil Aviation Flight University of China, Guanghan 618307, China

Received 10 February 2017; accepted 21 March 2017

Abstract

Inverse technique is a widely used method in oceanography, but it has a problem that the retrieved solutions often violate model prior assumptions. To tune the model has consistent solutions, an iteration approach, which successively utilizes the posterior statistics for next round inverse estimation, is introduced and tested from a real case study. It is found that the consistency may become elusive as the determinants of solution and noise covariance matrices become zero in the iteration process. However, after several steps of such operation, the difference between posterior statistics and the model prior ones can be gradually reduced.

Key words: regularization, consistency, inverse problems, box inverse model, L-curve method

Citation: Wei Yanzhou, Kang Xianbiao, Pei Yuhua. 2017. A case study of the consistency problem in the inverse estimation. Acta Oceanologica Sinica, 36(9): 45–51, doi: 10.1007/s13131-017-1110-3

1 Introduction

Inverse technique is a widely used method in earth sciences. For instance, it can be used to estimate ocean current (e.g., Wunsch, 1978; Yuan et al., 1992; Zhu et al., 2006), ocean mixing coefficients (e.g., Zika et al., 2010; Groeskamp et al., 2014), and geoacoustic parameters (e.g., Constable et al., 1987; Dosso et al., 2006). Although application fields are different, one common issue in the inverse estimation is how to do regularization. Statistical regularization requires prior information about the covariance matrix of unknowns. However, in most cases the covariance matrix itself needs to be determined, and out of limited prior information, a simple form matrix is often assumed, such as diagonal or Toeplitz form.

When the covariance matrix is fixed, it can be used to solve the inverse problems. After solutions are obtained, the consistency between retrieved solutions and model prior assumptions needs to be checked. If they are inconsistent, it is necessary to go back to change the model prior statistics (mean and covariance matrix) and do the inverse calculation again (e.g., McIntosh and Rintoul, 1997; Scales and Snieder, 1997). However, it is unclear how to modify the model prior statistics in an effective way. In this study, the posterior statistics shall replace the prior ones and be used to do the next round of inverse calculation, and this process is repeated to examine the effect. All the analyses will be based on a real case that uses the box inverse model (Wei et al., 2013).

This study is arranged as follows: Section 2 gives a short description about the case study; Section 3 gives the regularization techniques that are used for inverse problems; Section 4 gives the results; and Section 5 gives conclusions and discussion.

2 Case study

2.1 *Box inverse model*

In the past, the direct observation of the ocean current was difficult and expensive. Therefore, oceanographers often chose to infer the ocean current from hydrographic conditions, which were relatively easier to measure. This way was feasible because the vertical gradient of velocity was linearly related to the horizontal gradient of the seawater density as inferred from the thermal wind relationship, while the seawater density can be calculated from temperature and salinity data (e.g., Fofonoff and Millard, 1983). That meant the relative velocity at a hydrographic section can be calculated if the observed temperature and salinity data were available.

Now, the geostrophic current at a hydrographic section can be written into a combination of two parts:

$$v_g(x,z) = v_0(x,z_0) + v_r(x,z), \tag{1}$$

where x and z denote horizontal and vertical coordinates; $v_g(x, z)$ denotes the geostrophic velocity normal to the x direction; $v_r(x, z)$ denotes the relative velocity component that can be detected from hydrographic data; and $v_0(x, z_0)$ denotes the reference velocity component at a vertical level z_0 that still needs to be determined.

The box inverse method is proposed by Wunsch (1978) to solve this problem by use of property conservations, e.g., mass balance. It requires hydrographic sections are enclosed like a box. The water is vertically divided into layers (labeled with 1, 2, ..., M from surface to bottom) by isopycnals, with assumption

Foundation item: The National Natural Science Foundation of China under contract Nos 41490644 and 41490640.
*Corresponding author, E-mail: weiyanzhou@sio.org.cn

that no flux can penetrate through the isopycnals. Then the conservation of property fluxes (e.g., mass flux) in each layer leads to a system of linear equations for the reference velocity at each hydrographic section, i.e.,

$$\oint_L \int_{Z_i}^{Z_{i-1}} \rho(x,z)\cdot(v_r+v_0)\mathrm{d}z\mathrm{d}x = 0, \qquad i=1,2,\cdots,M, \quad (2)$$

where L denotes the line enclosed by the hydrographic sections; Z_i and $Z_{i\text{-}1}$ denote the depths of the lower and upper isopycnals of the ith layer; and ρ denotes the density. Discretization of Eq. (2) leads to:

$$\sum_{j=1}^{N}\rho_{i,j}\cdot(v_0)_j\cdot h_{i,j}\cdot\delta x_j = -\sum_{j=1}^{N}\rho_{i,j}\cdot(v_r)_{i,j}\cdot h_{i,j}\cdot\delta x_j = c_i,$$
$$i=1,2,\cdots,M, \quad (3)$$

where N denotes the number of station pairs; $\rho_{i,j}$ denotes the density at the ith layer and station pair j; $(v_0)_j$ denotes the reference velocity at station pair j; $(v_r)_{i,j}$ denotes the relative velocity at the ith layer and station pair j; $h_{i,j}$ denotes the thickness of the ith layer at station pair j, and δx_j denotes the distance between the jth pair of stations. Let $\boldsymbol{A}_0=(\rho_{i,j}\cdot h_{i,j}\cdot\delta x_j)_{M\times N}$, $\boldsymbol{v}_0=((v_0)_j)_{N\times 1}$, $\boldsymbol{c}_0=(c_i)_{M\times 1}$. Now Eq. (3) can be written in a concise form:

$$\boldsymbol{A}_0\times\boldsymbol{v}_0=\boldsymbol{c}_0, \quad (4)$$

where $\boldsymbol{A}_0$ is an $M\times N$ coefficient matrix, $\boldsymbol{v}_0$ is an $N\times 1$ column vector, and $\boldsymbol{c}_0$ is an $M\times 1$ column vector. Note that M indicates the number of layers, while N denotes the number of station pairs.

Both $\boldsymbol{A}_0$ and $\boldsymbol{c}_0$ are divided by the reference density 1 025 kg/m^3 into $\tilde{A}_0$ and $\tilde{c}_0$. Then, the mass conservation equations are represented in volume balance, and Eq. (4) is changed to

$$\tilde{\boldsymbol{A}}_0\times\boldsymbol{v}_0=\tilde{\boldsymbol{c}}_0. \quad (5)$$

Consider the noise in the ocean, a strict balance on mass is unrealistic. Therefore, Eq. (5) is modified by adding an uncertainty term $\boldsymbol{n}$:

$$\tilde{\boldsymbol{A}}_0\times\boldsymbol{v}_0=\tilde{\boldsymbol{c}}_0+\boldsymbol{n}. \quad (6)$$

Write a diagonal matrix $\boldsymbol{W}$ with $w_{j,j}=\Delta_j\cdot h_j$, where Δ_j and h_j denote the distance between the jth pair of stations and the water depth there. Let $\boldsymbol{A}=\tilde{\boldsymbol{A}}_0\boldsymbol{W}^{-1}$, $\boldsymbol{b}=\boldsymbol{W}\boldsymbol{v}_0$, $\boldsymbol{c}=\tilde{\boldsymbol{c}}_0$. Then Eq. (6) can be written as

$$\boldsymbol{A}\times\boldsymbol{b}=\boldsymbol{c}+\boldsymbol{n}. \quad (7)$$

Now the matrix $\boldsymbol{A}$ is dimensionless; $\boldsymbol{b}$, $\boldsymbol{c}$, and $\boldsymbol{n}$ are in the unit of 10^6 m^3/s. $\boldsymbol{b}$ denotes the barotropic volume transport contributed by the reference velocity v_0.

2.2 *Real case study*

In order to discuss the consistency problem in the inverse estimation, a real case study is employed here. That is about estimating reference velocity in two famous sections transecting the Kuroshio Current in the East China Sea (Fig. 1) (Wei et al., 2013, 2015). Temperature and salinity fields in the Sections PN and TK during 1987–2010 are observed by the Japan Meteorological Agency. They are processed to be in the identical spatial resolution in each section, i.e., 16 stations in the Section PN and 12 stations in the Section TK.

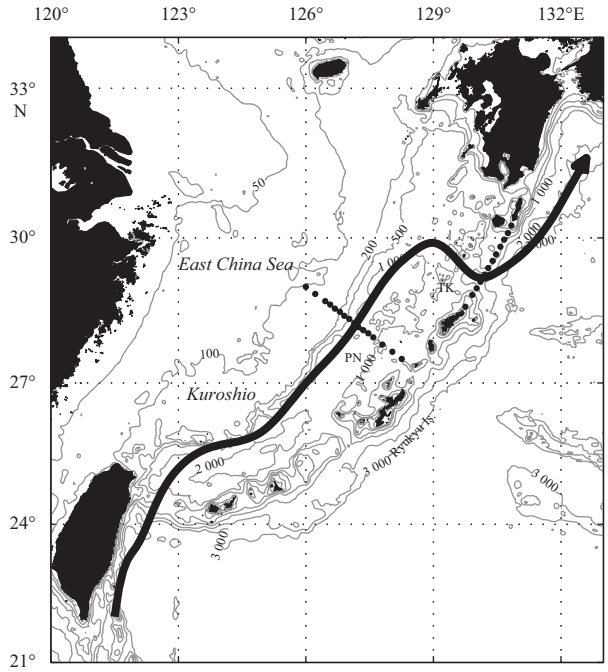

Fig. 1. Schematic map of the Kuroshio path and the locations of the Sections PN and TK. The grey thin lines with numbers denote the isobaths.

As confined by the continental slope and the island chain, most of the water transports through the Section PN will pass through the Section TK. Therefore, mass balance constraint can be imposed in these two sections (e.g., Zhu et al., 2006; Wei et al., 2013). The data at the Sections PN and TK are paired according to the availability of data in the two sections in the same season of a year. At last, 105 pairs are obtained during 1987–2010.

The water body is divided into five layers by 24.5, 25.5, 26.5 and 27.2σ_θ isopycnals in accordance to the work by Zhu et al. (2006), with almost equal thickness in each layer (Fig. 2). The layer beneath 27.2σ_θ is abandoned, and the other four layers are labeled by 1, 2, 3 and 4 from surface to bottom. The inward and outward mass fluxes in each layer are assumed to be conserved. Therefore, M=4 (which indicates the number of layers used for restriction) and N=15+11 (where 15 indicates the number of station pairs in the Section PN and 11 indicates the number of station pairs in the Section TK).

The bottom is chosen as the reference level, because the velocity there is close to 0 and its variance is small in common sense. For a single cruise study, a level that can lead to least initial imbalance can be the choice (e.g., Fiadeiro and Veronis, 1982; Yuan et al., 1992; Liu and Yuan, 1999). If there is surface shipboard ADCP observation, the observed surface velocity can be also used as a reference velocity (e.g., Nakano et al., 1994), but a pseudo strong current in the deep layer may be generated. The choice of a deep reference level also has its problem, as the estimated surface current does not match the shipboard ADCP velocity. That is because the thermal wind relationship is not highly precise for one cruise synoptic observation. However, choosing a reference level at surface is still unfavorable, because the variance of current is large there and can thus increase the variance of velocity in other levels. Basically, the level where the mean velocity struc-

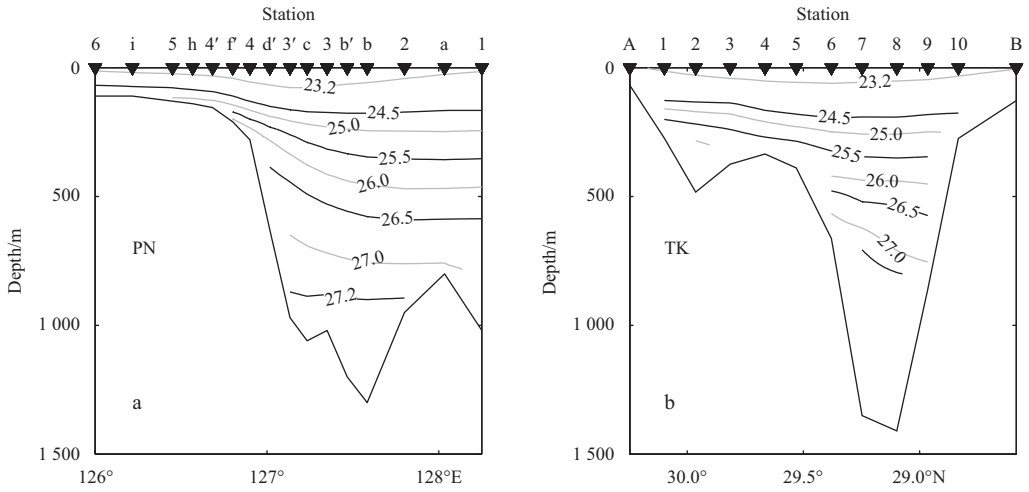

Fig. 2. Climatology mean potential density in Sections PN (a) and TK (b). The bold black lines indicate the interfaces of the five layers used in the box inverse model. The inverted triangles with labels on the top of each panel indicate the positions and names of stations.

ture is well known, and the variance of current is smaller is the best choice for the long term estimation. Here, the bottom level is subjectively considered to satisfy this condition.

3 Regularization

3.1 *Tikhonov regularization and parameter choice rule*

In many cases, the matrix $\boldsymbol{A}$ in Eq. (7) is not well-posed, so that the solution $\boldsymbol{b}$ cannot be calculated in traditional ways. However, it can be obtained by using the Tikhonov regularization method (Tikhonov and Arsenin, 1977):

$$\boldsymbol{b} = \boldsymbol{A}^{\mathrm{T}} \left(\boldsymbol{A}\boldsymbol{A}^{\mathrm{T}} + a^2\boldsymbol{I}\right)^{-1} \boldsymbol{c}. \tag{8}$$

The parameter a^2 is called the regularization parameter, which reflects the ratio of model uncertainty to the size of solution (e.g., Hansen, 2001). $\boldsymbol{I}$ denotes unit matrix. This method is similar to the Levenberg-Marquardt algorithm (also known as damped least squares method) (Levenberg, 1944; Marquardt, 1963) and the ridge regression (e.g., Hoerl and Kennard, 2000). The Tikhonov regularization is often the best choice in case there is nothing information about the model prior statistics.

The regularization parameter a^2 is chosen to trade off the norms of solution and noise to be both acceptable small. The choice rules generally include the L-curve method (Hansen, 2001), the cross validation method (Golub et al., 1979), and the Morozov's discrepancy principle (e.g., Engl et al., 1996). Among them, the L-curve method, as a noise level free parameter choice rule, has gained popularity and is widely used.

Denote

$$\eta = \ln \|\boldsymbol{b}\|_2, \quad \rho = \ln \|\boldsymbol{n}\|_2. \tag{9}$$

The L-curve is a plot of η versus ρ. Notice that η and ρ are functions of a^2. Let η', ρ', η'', and ρ'' be the first and second derivatives of η and ρ with respect to a^2. Then the curvature κ of the L-curve, as a function of a^2, is given by

$$\kappa = 2\,\frac{\rho'\eta'' - \rho''\eta'}{\left((\rho')^2 + (\eta')^2\right)^{3/2}}. \tag{10}$$

The best a^2 corresponds to the knee point of the L-curve, or the maximum of the curvature κ. Note that the L-curve method cannot work for all the cases and has its limitation (Hansen, 2001).

3.2 *Statistical regularization*

The regularization problem has a general form, if there are prior statistics about both solution and model error (i.e., their expectations and covariance matrixes) (e.g., McIntosh and Rintoul, 1997; Snieder and Trampert, 1999; Tarantola, 2005). Given the mean and covariance matrix of solution $\boldsymbol{b}$ (denoted by $\bar{\boldsymbol{b}}$ and $\boldsymbol{C}_b$) and noise $\boldsymbol{n}$ (denoted by $\bar{\boldsymbol{n}}$ and $\boldsymbol{C}_n$), Eq. (7) can be written as

$$\boldsymbol{A} \times (\bar{\boldsymbol{b}} + \boldsymbol{b}') = \boldsymbol{c} + (\bar{\boldsymbol{n}} + \boldsymbol{n}'). \tag{11}$$

Now the solution to this inverse problem is

$$\boldsymbol{b} = \bar{\boldsymbol{b}} + \boldsymbol{b}' = \bar{\boldsymbol{b}} + \boldsymbol{C}_b\boldsymbol{A}^{\mathrm{T}} \left(\boldsymbol{A}\boldsymbol{C}_b\boldsymbol{A}^{\mathrm{T}} + \boldsymbol{C}_n\right)^{-1} \left(-\boldsymbol{A}\bar{\boldsymbol{b}} + \boldsymbol{c} + \bar{\boldsymbol{n}}\right), \tag{12}$$

and the corresponding noise term is

$$\boldsymbol{n} = \bar{\boldsymbol{n}} + \boldsymbol{n}' = \bar{\boldsymbol{n}} - \boldsymbol{C}_n \left(\boldsymbol{A}\boldsymbol{C}_b\boldsymbol{A}^{\mathrm{T}} + \boldsymbol{C}_n\right)^{-1} \left(-\boldsymbol{A}\bar{\boldsymbol{b}} + \boldsymbol{c} + \bar{\boldsymbol{n}}\right). \tag{13}$$

The solution in Eq. (12) minimizes the following function:

$$\chi^2 = \left(\boldsymbol{b} - \bar{\boldsymbol{b}}\right)^{\mathrm{T}} \boldsymbol{C}_b^{-1} \left(\boldsymbol{b} - \bar{\boldsymbol{b}}\right) + \left(\boldsymbol{n} - \bar{\boldsymbol{n}}\right)^{\mathrm{T}} \boldsymbol{C}_n^{-1} \left(\boldsymbol{n} - \bar{\boldsymbol{n}}\right). \tag{14}$$

In relative to the Tikhonov regularization, the statistical inversion gives a more precise depiction of the regularization problem. The Tikhonov regularization can be viewed as a simple form of the statistical inversion, with the prior statistics about the solution and model error implicitly assumed.

Denote $\boldsymbol{y}' = \begin{pmatrix} \boldsymbol{b}' \\ \boldsymbol{n}' \end{pmatrix}$ and $\boldsymbol{C}_y$ is the covariance matric of $\boldsymbol{y}'$, the optimum solution for Eq. (11) should minimize $\boldsymbol{y}'^{\mathrm{T}} \boldsymbol{C}_y^{-1} \boldsymbol{y}'$. Only when the noise $\boldsymbol{n}'$ is independent to the solution $\boldsymbol{b}'$, the solution that can minimize Eq. (14) is optimum. The independence between $\boldsymbol{n}'$ and $\boldsymbol{b}'$ is often subjectively assumed, but the discrepancy of this assumption should be awared of.

The noise term $\boldsymbol{n}$ in Eq. (11) is decomposed into two parts to emphasize the importance of the mean imbalance in each layer (caused by some source terms) for a precise estimation. Now it is evident from Eq. (12) that a successful estimation relies on sufficient information about the mean solution ($\bar{\boldsymbol{b}}$), mean noise ($\bar{\boldsymbol{n}}$), covariance matrix of solution ($\boldsymbol{C}_b$), and covariance matrix of noise ($\boldsymbol{C}_n$), and the independence assumption between $\boldsymbol{n}'$ and $\boldsymbol{b}'$ is correct. If the last one is not satisfied, even with accurate values of prior statistics, the estimated solution is not the best. As noticed by McIntosh and Rintoul (1997): "the statistical inverse method may not give the best solution for a particular inversion, even with accurate prior statistics. However, by design, it will give the solution with the least error over many realizations."

Some researchers have added other terms in the objective function to make the solutions have some physical meanings. For example, the smoothness of the solution, i.e., $\|\partial \boldsymbol{b}\|^2$, has been considered as an objective term of minimization (Constable et al., 1987); the total mass imbalance, i.e., $\left(\sum_{i=1}^{M} n_i\right)^2$ has been also considered as an objective term (Wei et al., 2013). These terms are not considered here for simplicity.

3.3 *Consistency*

After solutions are obtained from Eq. (12), consistency between retrieved solutions and model prior assumption should be checked. The consistency between model and retrieved solutions is measured by the distribution of χ^2 values calculated in Eq. (14). In a consistent estimation, the values follow the theoretical chi square (χ^2) distribution with M degrees of freedom (e.g., Tarantola, 2005). If statistics of the retrieved solutions violate the model prior assumption, the model prior statistics should be changed, as said by Scales and Snieder (1997), "In other words, in a succession of different inversions one tunes the a priori model statistics in such a way that the retrieved model has agreeable features. Note that in such an approach the a priori model statistics are used a posteriori to tune the retrieved model!" However, it is unclear how to tune the model effectively to produce consistent solutions. This study shall take the statistics of the retrieved solutions as the model prior statistics to solve the inverse problems again, and repeat this process to see the effect.

4 Experiment and results

An experiment is carried out to discuss the consistency problem as mentioned above. In general, as the prior statistics about the solution and the model error are unknown, the Tikhonov solution is often the best choice. Written in Eqs (11)–(13), the initial choices of $\bar{\boldsymbol{b}}$ and $\boldsymbol{C}_b$ are $\bar{\boldsymbol{b}} = 0$ (correspondingly, $\bar{\boldsymbol{v}}_0 = \boldsymbol{W}^{-1}\bar{\boldsymbol{b}} = 0$) and $\boldsymbol{C}_b = \boldsymbol{I}_{26\times26}$; the choices of $\bar{\boldsymbol{n}}$ and $\boldsymbol{C}_n$ are $\bar{\boldsymbol{n}} = [0.7, 0, 0, 0]^{\mathrm{T}}$ and $\boldsymbol{C}_n = a^2 \times \boldsymbol{I}_{4\times4}$. Here $\bar{n}_1 = 0.7$ is used to account for the Kuroshio onshore intrusion before transporting through the Section TK (Wei et al., 2013). a^2 is the regularization parameter. a^2=1.0 means the objective function (14) stands for the barotropic volume transport contribution (unit: 10^6 m^3/s) by reference velocity $\boldsymbol{v}'_0$, and the mass imbalance components $\boldsymbol{n}'$ (unit: 10^6 m^3/s) are both small. Therefore, it can be directly chosen to be a^2=1.0 following this physical implication, or chosen following the L-curve rule (see Section 4.1). Moreover, unlike that treated by Wei et al. (2013) and Zhu et al. (2006), the solution and the model error are not constrained in this study. Note the difference between the Tikhonov solutions and the solutions obtained from a constrained optimization. In this case, no Tikhonov type solution can be obtained to satisfy the conditions that the absolute value of each component is less than 0.2 m/s and the imbalance at Layers 2–4 are less than 0.5×10^6 m^3/s simultaneously for all the 105 cases, but such solutions do exist for the constrained optimization (Wei et al., 2013).

After the solution $\boldsymbol{b}$ and noise $\boldsymbol{n}$ for all the 105 cases are obtained, the posterior statistics $\bar{\boldsymbol{b}}$, $\boldsymbol{C}_b$, $\bar{\boldsymbol{n}}$ and $\boldsymbol{C}_n$ can be calculated. These posterior statistics are then used as the model prior statistics to do the next round of inverse calculation. This process is carried out repeatedly to examine whether the model converges (posterior statistics are close to the prior statistics) like that of seeking the root of a function using Newton's method.

4.1 *Regularization parameter obtained by the L-curve method*

In this subsection, the Tikhonov regularization parameters are determined by the L-curve rule. Figures 3a–c show an example of the solution norm and residual norm plots versus a^2, the L-curve plot, and the curvature of the L-curve. The red points in Figs 3a and b indicate the values calculated from the optimum a^2, which corresponds to the largest curvature κ in L-curve (Fig. 3c). Note that the L-curve method is not applicable to all cases

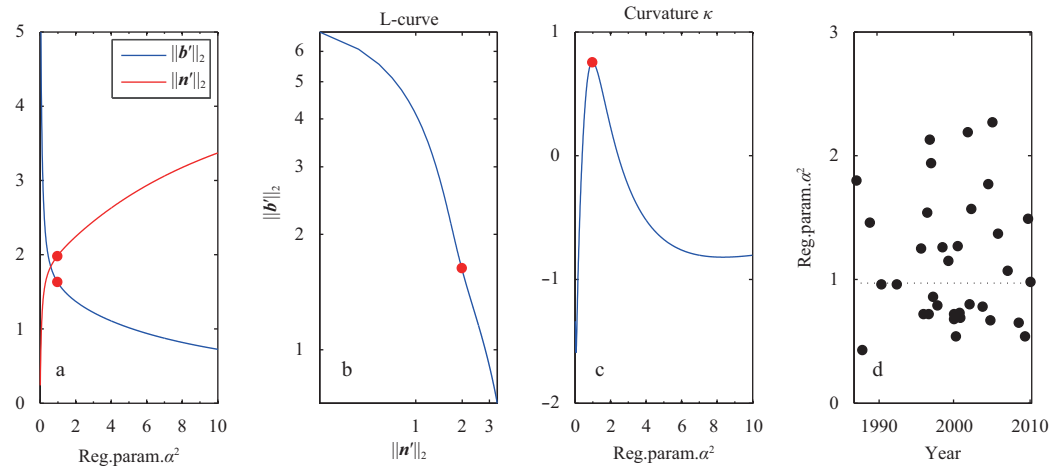

Fig. 3. An example of the solution norm and residual norm plots versus regularization parameter a^2 (a), the L-curve plot (b), and the curvature κ of the L-curve versus a^2. The red points in these figures denote the values correspond to the optimum a^2 determined following the L-curve rule. The a^2 values determined from the L-curve method during 1987–2010 are plotted in panel (d). The dash line in Fig. 3d denotes the median value of a^2.

(Hansen, 2001). For some cruises in this study, there is even no convex corner in the corresponding L-curves (i.e., the κ is always negative). Here, the optimum a^2 are collected and plotted in Fig. 3d, when positive κ is available like that in Fig. 3c. As evident from Fig. 3d, the a^2 generally varies from 0.5 to 2.0 with a mean (median) value of 1.13 (0.97). This value is quite close to 1.0, so that guarantees the barotropic volume transport (contributed by reference velocity departure $\boldsymbol{v}'_0$) and the mass imbalance departure component $\boldsymbol{n}'$ are both small. Therefore, in accordance to both the L-curve rule and this physical implication, the regularization parameter can be chosen to be a^2=1.0.

4.2 *Effect by successively tuning model with posterior statistics*

Initialized with the Tikhonov solution (a^2=1.0), the posterior statistics can be obtained and then used as model prior statistics to solve the inverse problems again. Initially, the objective function (14) equals to $\|\boldsymbol{b}'\|^2 + \|\boldsymbol{n}'\|^2$, which means the barotropic contribution (1×10^6 m^3/s) by the reference velocity departures and the mass imbalance components departures (1×10^6 m^3/s) are both small. Figure 4 shows the statistics about $\bar{\boldsymbol{v}}_0$, $\boldsymbol{C}_b$, $\bar{\boldsymbol{n}}$, $\boldsymbol{C}_n$, and the Kuroshio volume transport (KVT) in two sections calculated after each step of inversion. $\bar{\boldsymbol{v}}_0$, instead of $\bar{\boldsymbol{b}}$, is shown here, because $\bar{\boldsymbol{v}}_0$ is easier to understand.

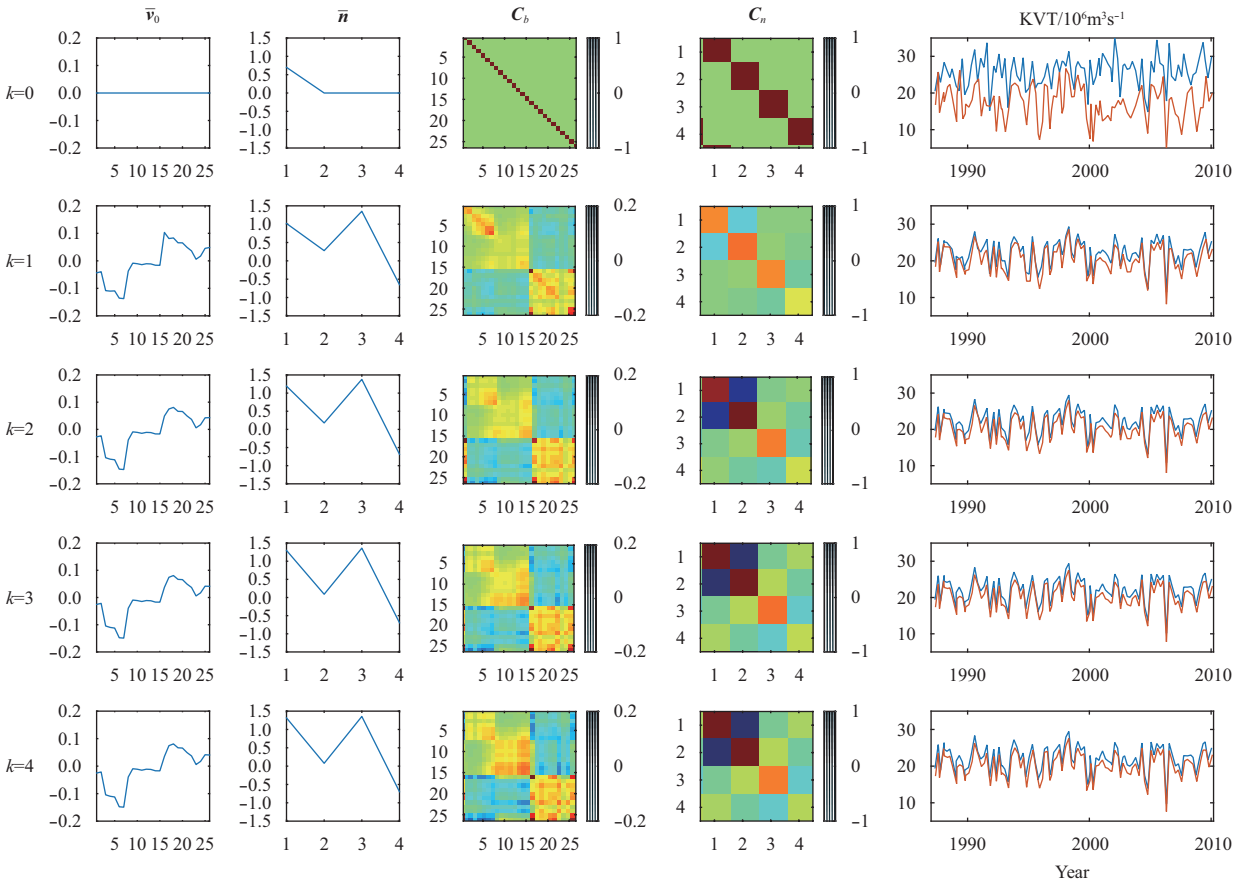

Fig. 4. The initial statistics (first row) and statistics estimated after the kth inversion (k+1 row) for the mean reference velocity (first column), mean mass imbalance (second column), covariance matrix of solution $\boldsymbol{b}$ (third column), covariance matrix of model noise $\boldsymbol{n}$ (forth column), and the KVT (last column; the blue lines denote the KVT values in the Section PN and red lines denote that in the Section TK).

The inconsistency between the model prior and posterior statistics can be seen through comparing the values in the second row to that in the first row (Fig. 4). The degree to which they are consistent can be evaluated by comparing the distribution of χ^2 values calculated from Eq. (14) to the theoretically chi square distribution (four degrees of freedom; e.g., Tarantola, 2005) (Fig. 5). The overlapped area between two distributions (Fig. 5) indicates how much they are consistent. From Fig. 5, it can be seen that the model prior statistics and the retrieved solutions are not highly consistent. That means the model prior statistics implicitly assumed in the Tikhonov solution need to be modified to increase the consistency.

In order to tune the model to have consistent solutions, the posterior statistics generated in the first round of inversion (k=1) are used as the model prior statistics for the next round calculation. This process is repeated. Figure 4 shows that the differences between the prior statistics and the regenerated posterior statistics can be gradually reduced, and the model statistics become stable. For example, Fig. 6a shows the difference between the retrieved solution mean $\bar{\boldsymbol{b}}$ at the kth iteration step and (k-1)th iteration step. It can be seen that the difference decreases as iteration step k increases. Figure 6b shows the root mean square difference between the retrieved solution $\boldsymbol{b}$ at the kth iteration step and (k-1)th iteration step. It can be seen that the difference decreases as iteration step k increases. Note that the final statistics highly rely on the initial choice of the model prior statistics.

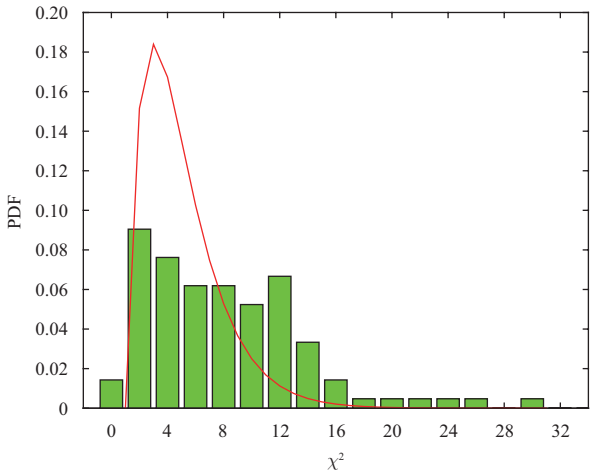

Fig. 5. Comparison of the probability density function (PDF) of the calculated χ^2 values from the real case study (green bars) and that from the theoretical chi square distribution with four degrees of freedom (red line).

The consistency between the model prior statistics and the retrieved solution in a strictly statistic sense is still difficult to evaluate, because the determinants of $\boldsymbol{C}_b$ and $\boldsymbol{C}_n$ are close to 0, so that the χ^2 values in Eq. (14) cannot be calculated after the first round simple Tikhonov regularization.

5 Concluding remarks

The consistency problem in the inverse estimation is discussed from a real case study. It is seen that the retrieved Tikhonov solutions do not necessarily agree with the model prior statistics, and the degree to which they are consistent can be measured by the overlapped area between the distribution of calculated χ^2 values (Eq.(14)) and the theoretical chi-square distribution (e.g., Fig. 5).

If taking the posterior statistic as the model prior statistics for next round of inverse estimation, the regenerated posterior statistics may gradually match to the prior ones. The success of this procedure relies on the use of Eqs (12) and (13) help to avoid direct calculation of the inverse of $\boldsymbol{C}_b$ and $\boldsymbol{C}_n$, whose determinants are close to 0 in the iteration process. However, the consistency in statistics is still elusive, because the χ^2 values in Eq. (14) cannot be calculated when the determinants of $\boldsymbol{C}_b$ and $\boldsymbol{C}_n$ are 0.

Nevertheless, current study provides a way that might be used to reduce the difference between the statistical values of the model prior assumption and the retrieved solutions. There are still some problems need to be solved, such as in which cases the iteration approach can converge, and how to evaluate the consistency in case the determinants of $\boldsymbol{C}_b$ and $\boldsymbol{C}_n$ are 0.

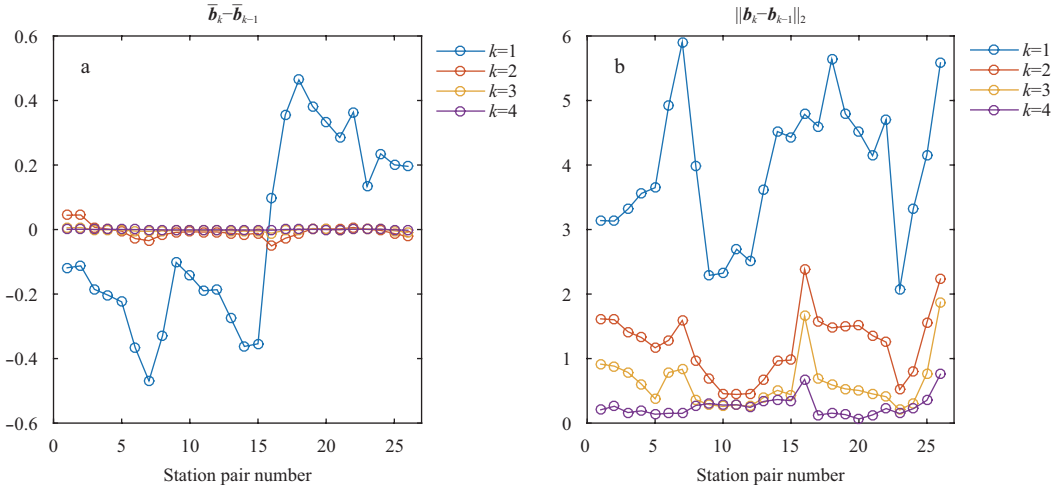

Fig. 6. The difference between the retrieved solution mean $\bar{\boldsymbol{b}}$ at the kth iteration step and (k-1)th iteration step (a), and the root mean square difference between the retrieved solution $\boldsymbol{b}$ at the kth iteration step and (k-1)th iteration step (b).

References

Constable S C, Parker R L, Constable C G. 1987. Occam's inversion: a practical algorithm for generating smooth models from electromagnetic sounding data. Geophysics, 52(3): 289–300

Dosso S E, Nielsen P L, Wilmut M J. 2006. Data error covariance in matched-field geoacoustic inversion. J Acoust Soc Am, 119(1): 208–219

Engl H W, Hanke M, Neubauer A. 1996. Regularization of Inverse Problems. Dordrecht: Kluwer Academic Publishers, 322

Fiadeiro M E, Veronis G. 1982. On the determination of absolute velocities in the ocean. J Mar Res, 40: 159–182

Fofonoff N P, Millard Jr R C. 1983. Algorithms for computation of fundamental properties of seawater. Paris: UNESCO Technical Paper in Marine Science, 44: 1–53

Golub G H, Heath M, Wahba G. 1979. Generalized cross-validation as a method for choosing a good ridge parameter. Technometrics, 21(2): 215–223

Groeskamp S, Zika J D, Sloyan B M, et al. 2014. A thermohaline inverse method for estimating diathermohaline circulation and mixing. J Phys Oceanogr, 44(10): 2681–2697

Hansen P C. 2001. The L-curve and its use in the numerical treatment of inverse problems. In: Johnston P, ed. Computational Inverse Problems in Electrocardiology: Advances in Computational Bioengineering, Vol. 5. Southampton: WIT Press, 119–142

Hoerl A E, Kennard R W. 2000. Ridge regression: biased estimation for nonorthogonal problems. Technometrics, 42(1): 80–86

Levenberg K. 1944. A method for the solution of certain non-linear problems in least squares. Quart Appl Math, 2(2): 164–168

Liu Yonggang, Yuan Yaochu. 1999. Variability of the Kuroshio in the East China Sea in 1992. Acta Oceanologica Sinica, 18(1): 1–15

Marquardt D W. 1963. An algorithm for least-squares estimation of nonlinear parameters. J Soc Indust Appl Math, 11(2): 431–441

McIntosh P C, Rintoul S R. 1997. Do box inverse models work? J Phys

Oceanogr, 27(2): 291–308
Nakano T, Takatsuki Y, Kaneko I. 1994. The Kuroshio structure and transport estimated by the inverse method. J Phys Oceanogr, 24(3): 609–618
Scales J A, Snieder R. 1997. To Bayes or not to Bayes? Geophysics, 62(4): 1045–1046
Snieder R, Trampert J. 1999. Inverse problems in geophysics. In: Wirgin A, ed. Wavefield Inversion. Vienna: Springer-Verlag, 119–190
Tarantola A. 2005. Inverse Problem Theory and Methods for Model Parameter Estimation. Philadelphia, Pennsylvania: SIAM, 342
Tikhonov A N, Arsenin V Y. 1977. Solutions of Ill-Posed Problems. John F, Trans. Washington, D C: V H Winston & Sons, 258
Wei Yanzhou, Huang Daji, Zhu Xiaohua. 2013. Interannual to decadal variability of the Kuroshio Current in the East China Sea from 1955 to 2010 as indicated by in-situ hydrographic data. J Oceanogr, 69(5): 571–589
Wei Yanzhou, Pei Yuhua, Zhang Ronghua. 2015. Seasonal variability of the Kuroshio Current at the Section PN in the East China Sea based on *insitu* observation from 1987 to 2010. Acta Oceanologica Sinica, 34(5): 12–21
Wunsch C. 1978. The North Atlantic general circulation west of 50°W determined by inverse methods. Rev Geophys, 16(4): 583–620
Yuan Yaochu, Su Jilan, Pan Ziqin. 1992. Volume and heat transports of the Kuroshio in the East China Sea in 1989. La mer, 30(3): 251–262
Zhu Xiaohua, Park J H, Kaneko I. 2006. Velocity structures and transports of the Kuroshio and the Ryukyu current during fall of 2000 estimated by an inverse technique. J Oceanogr, 62(4): 587–596
Zika J D, McDougall T J, Sloyan B M. 2010. A tracer-contour inverse method for estimating ocean circulation and mixing. J Phys Oceanogr, 40(1): 26–47